Preparation and Characterization of a Polycaprolactone/C_{60} Composite and its Improved Counterpart (PCL—NH_2/C_{60}—OH)

Chin-San Wu

Department of Chemical and Biochemical Engineering, Kao Yuan University, Kaohsiung County, Taiwan 82101, Republic of China

Received 12 December 2008; accepted 25 May 2009
DOI 10.1002/app.30833
Published online 4 November 2009 in Wiley InterScience (www.interscience.wiley.com).

ABSTRACT: In this study, polycaprolactone/C_{60} (PCL/C_{60}) hybrids were prepared via a melt-blending method. To enhance the compatibility between PCL and C_{60}, the acrylic acid-grafted polycaprolactone (PCL-*g*-AA) was first transformed to PCL—NH_2 by mixing with 1,6-diaminohexane, while C_{60} was oxidized using a mixture of H_2SO_4/HNO_3 and NaOH to derive C_{60} fullerol (C_{60}—OH). Thereafter, C_{60}—OH and PCL—NH_2 were used to replace PCL and C_{60}, respectively. The resulting products were characterized using FTIR, solid-state ^{13}C- and ^{1}H- NMR, TGA, DMA, SEM, TEM, and Instron mechanical testing. Because of the formation of —NHCO groups through the reaction between amino groups of PCL—NH_2 and hydroxyl groups of C_{60}—OH, thermal and mechanical properties of the PCL—NH_2/C_{60}—OH composite were significantly superior to those of PCL/C_{60}. The optimal blend was the 5 wt % C_{60}—OH with PCL—NH_2, producing an 84°C increase in initial decomposition temperature (IDT). C_{60}—OH in excess of 5 wt % aggregated and caused separation of the organic and inorganic phases, lowering their compatibility.
 J Appl Polym Sci 115: 3489–3499, 2010

Key words: polyesters; NMR; blended; compatibility

INTRODUCTION

Because of its promising physical, thermal, mechanical, and electrical properties, C_{60} fullerene has attracted extensive scientific interest recently.[1–5] Moreover, applications of C_{60} fullerene in structural materials such as polymer composites become more feasible as their mass production leads to price reduction.[6,7] Of particular interest is the use of C_{60} in polymer/C_{60} composites,[8,9] as reports indicate that matrix properties can be effectively enhanced via its addition.[10,11] However, aggregation and nonuniform dispersion of C_{60} filler in common polymer matrix can be an issue, and therefore two primary conditions are required for the application of C_{60} composites: the homogeneous dispersion of C_{60} in the host matrix and appropriate interfacial interaction. Recently, various methods have been introduced for functionalizing C_{60} to improve its compatibility with monomers and polymers.[12,13] Of these methods, most involve oxidation of the surfaces of C_{60},[14–16] such as oxidation of C_{60} in a mixture of sulfuric and nitric acids or by treatment with piranha (sulfuric acid/hydrogen peroxide). In a mixture of strong oxidizing acids such as HNO_3 or H_2SO_4,[10,17,18] C_{60} can be functionalized with carboxyls or quinines. The dispersion of oxidized C_{60} in solvents or polymer matrices can be further enhanced by the grafting of organic polymers onto their surfaces. Ma et al.[19] described the efficacy of functionalized phenolic resin blended with polyurethane/C_{60}—OH copolymer. The various methods proposed include either growing polymers from negatively charged C_{60} or anchoring polymers onto chemically oxidized C_{60}.

The use of nonrenewable petroleum-based chemicals for the synthesis and manufacture of commercial polymers has caused many environmental problems associated with their disposal. The main strategies to address these problems are the utilization of polymeric materials from renewable sources such as starch, cellulose, and wood flour, and the development of biodegradable polymeric materials such as polylactic acid (PLA), polycaprolactone (PCL), and poly(3-hydroxybutyrate) (PHB). PCL is one of the most important thermoplastics but its use is restricted to certain applications by its low melting point, low stability in hydrocarbons, and a tendency to crack when stressed.[20,21] Attempts over many years to mitigate these problems have focused on grafting reaction, crosslinking reaction, and blending with organic fillers.

Correspondence to: C.-S. Wu (cws1222@cc.kyu.edu.tw).

In this study, a PCL/C_{60} composite was prepared to combine the qualities of these materials. Furthermore, amino-grafted PCL (PCL—NH_2) and hydroxyl group-functionized C_{60} (C_{60}—OH) were also synthesized and covalently linked to obtain an even more promising material (PCL—NH_2/C_{60}—OH). Thereafter, PCL/C_{60} and PCL—NH_2/C_{60}—OH were thoroughly characterized by Fourier transform infrared (FTIR) spectroscopy, scanning electron microscopy (SEM), solid-state ^{1}H- and ^{13}C-NMR, Instron mechanical testing, and thermal analysis techniques to compare their performance.

EXPERIMENTAL

Materials

The commercial-grade PCL (CAPA 6800), with a molar mass of 80,000 g/mol, was supplied by Solvay Chemicals (Warrington, United Kingdom). The fullerenes (C_{60}, purity >98%), sulfuric acid (96%), nitric acid (61%), and 1,6-diaminohexane were purchased from Aldrich Chemical (Milwaukee, WI). Acrylic acid (AA; Aldrich Chemical) was purified before use by recrystallization from chloroform. The initiator dicumyl peroxide (DCP; Aldrich Chemical) was recrystallized twice by dissolving it in absolute methanol. Other reagents were purified using the conventional methods. The PCL-*g*-AA copolymer was made in our laboratory according to the procedures described in our previous work,[22] and its grafting percentage was approximately 6.05 wt %. The PCL-*g*-AA samples in a chloroform solvent and the catalyst Sb_2O_3 were mixed with 1,6-diaminohexane at 100–110°C for 24 h under refluxing N_2 to convert the carboxyls into amino groups, and this produced the amino group-functionalized PCL (namely, PCL—CONH—$(CH_2)_6$—NH_2, designated as PCL—NH_2).

Preparation of PCL—NH_2/C_{60}—OH Hybrids

Scheme 1 illustrates the route for synthesizing PCL—NH_2/C_{60}—OH. The C_{60} was first chemically oxidized with a strong oxidizing agent (a 3 : 1 concentrated H_2SO_4/HNO_3 mixture) at 120–130°C for 12 h to generate carboxyl groups. The acid-treated samples were then quenched with ice made from distilled water. The resulting mixture was filtered to remove insoluble particles. It was subsequently neutralized by slowly adding NaOH solution (2*M*). During this reaction, the solution turned from yellow to dark brown, and a fine brown powder was formed at pH 12–13. The powder was separated from the solution by settling overnight and decanting, and it was then washed with NaOH solution (1*M*) and centrifuged. This washing was repeated three times, and the powder was then washed for further three times with methanol (99%; Aldrich) and dried under primary vacuum for 24 h at 105°C. It was then purified by dissolving in HCl solution (0.2*M*). This acid solution was neutralized by adding NaOH solution (1*M*) (adjusted to pH 12–13). At this stage, no precipitation occurred. A precipitate was obtained by treating the solution with acetonitrile (99.5%; Aldrich). A final further washing of the precipitate three times with methanol and drying for 72 h under primary vacuum produced a brown powder product. Before blending with PCL—NH_2, the C_{60}—OH was dried again in a vacuum oven at 105°C for 2 days.

Having prepared PCL—NH_2 and C_{60}—OH separately, the PCL—NH_2/C_{60}—OH composites were then blended using a Brabender "Plastograph" 200 Nm W50EHT mixer with a blade-type rotor. The rotor speed was set at 50 rpm, and the blending reaction was catalyzed by Sb_2O_3 and carried out at 100°C for 40 min. The mass ratios of C_{60}—OH to PCL—NH_2 were set at 1/99, 3/97, 5/95, 7/93, and 10/90. After blending, the composite was pressed

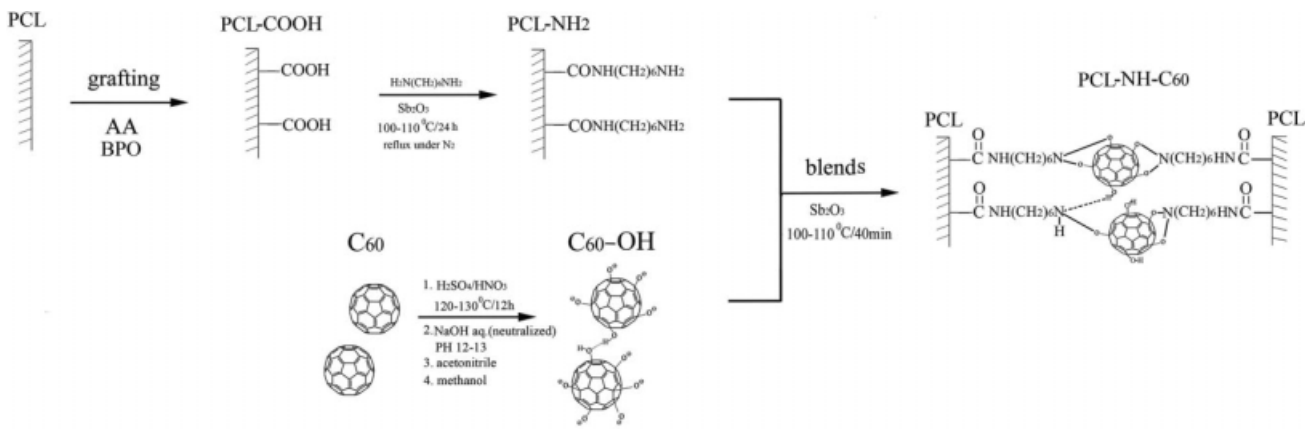

Scheme 1 Reaction scheme for the modification of C_{60} and PCL and the preparation of blends.

into 1-mm-thick plates using a hydraulic press at 100°C and then put into a dryer for cooling. The cooled plates were made into standard specimens for further characterization. The relative humidity of the desiccator was set at 50% ± 5%, and then the samples were conditioned for 24 h. We found that 24 h of conditioning was adequate for dehydrating samples to appropriate water content and that a longer storage time did not have an appreciable effect on composite properties.

Characterization of hybrids

FTIR spectrometry (BIO-RAD FTS-7PC type) was used to investigate the grafting reaction of the amino group onto PCL and to verify the incorporation of a C_{60}—OH phase to the extent that amide bonds were formed in hybrids. For the FTIR tests, the sample was ground into a fine powder by the milling machine and then pressed into pellets with KBr. The solid-state ^{1}H- and ^{13}C-NMR analysis was performed using a Bruker AMX 400 NMR spectrometer at the condition of 50 MHz. The NMR spectra were observed under crosspolarization; magic antic angle sample spinning and power decoupling conditions with 90° pulse and 4s cycle time. For DSC tests, sample sizes ranged from 4 to 6 mg, and the T_g and T_m values were obtained from the melting curves taken at a temperature range of −30 to 120°C, scanned at a heating rate of 10°C/min. To evaluate the compatibility of blends, the dynamic mechanical properties of blends were assessed in a TA analyzer Model 2080 (New Castle, DE). The tests were performed at a frequency of 1 Hz, a strain level of 0.075%, and a temperature range of −100 to 100°C with a heating rate of 3°C/min. The static force, which is in the linear region of elasticity and without causing drawing effects, was specified via several stress–strain experiments performed beforehand, and the ratio of static force to dynamic force was kept constant during the experiments. Thermogravimetry analysis (TA Instrument 2010 TGA, New Castle, DE) was used to assess whether organic–inorganic phase interactions influenced thermal degradation of hybrids. The samples were placed in alumina crucibles and tested with a thermal ramp over the temperature range of 30 to 600°C at a heating rate of 20°C/min, and then the IDTs of hybrids were obtained. An XL-40FEG SEM (Philips, The Netherlands) was used to study the morphology of the hybrids. Before testing, hybrids were prepared as thin films with a hydraulic press, and then the films were treated with hot water at 80°C for 24 h. Then, they were coated with gold and observed under the SEM. Additionally, a micrograph of a microtome section of the hybrids of 60–100 nm thickness, mounted in epoxy resin, was produced using a transmission electron microscope (JEM-100CX II, Jeol Company, Japan) at an acceleration voltage of 100 kV. Mechanical testing was performed according to the ASTM D 638 method; an Instron mechanical tester (Model LLOYD, LR5K type) was used to measure the tensile strength and strain at break. The films of test samples, which were conditioned at 50% ± 5% relative humidity for 24 h before the measurements, were prepared in a hydraulic press at 100°C, and then the analysis was performed at a 20 mm/min crosshead speed. Five measurements were taken for each sample and the results were averaged to obtain a mean value.

RESULTS AND DISCUSSION

FTIR/NMR analysis

Figure 1 shows the FTIR spectra of PCL (Line A) and PCL-*g*-AA (Line B). In addition to the characteristic peaks[23,24] at 3300–3700, 1725, 852–1480, and 720 cm^{-1} observed in both polymers, there exists an obvious extra peak at 1710 cm^{-1} for the modified PCL. This extra peak, characteristic of —C=O, and the broad —OH stretching absorbance at 3200–3700 cm^{-1} indicates the presence of free acid in the modified polymer. The FTIR spectrum of compound obtained from the reaction of PCL-*g*-AA and 1,6-diaminohexane (namely, PCL—NH_2) is also shown in Figure 1(C). This spectrum shows additional unique absorption peaks at 1660 cm^{-1}, and these are assigned to —C=O of —CONHR. This amide functional group is formed via the reaction between —COOH of PCL-*g*-AA and —NH_2 of 1,6-diaminohexane when the two compounds are blended. Furthermore, in addition to the peaks characteristic of C—N and NH_2 in —$CONH_2$ (at 1088 cm^{-1} and 878 cm^{-1}, respectively), the PCL—NH_2 spectrum identifies differences in absorbance intensity at 1628 cm^{-1} (amide I, secondary amide) and 1582 cm^{-1} (nonacylated primary amino),[25] both of which further illustrate the reaction between 1,6-diaminohexane and PCL-*g*-AA. Additionally, spectrum C shows that peaks at 3200–3600 cm^{-1} are much more intense than the stretching absorbance at 3000–3600 cm^{-1} in Spectrum B. It is proposed that these more intense peaks are caused by the —NH_2 group of PCL—NH_2.

C_{60}—COOH was obtained from the chemical oxidation of C_{60} by the strong oxidizing acid [(96%)H_2SO_4/(65%)HNO_3 = 1/3], and the FTIR spectrum is shown in Figure 2(B). Similar to the findings of Huang et al.,[26] all the characteristic peaks of C_{60}—COOH appeared at 1181 cm^{-1} and 1352 cm^{-1} (C—O), 1600–1450 cm^{-1} (aromatic ring), 1722 cm^{-1} (C=O), and 3396 cm^{-1} (—OH). The FTIR spectrum of C_{60} [Fig. 2(A)] does not show the peak at 1722 cm^{-1}, demonstrating the chemical oxidation that cleaves the long ropes of C_{60} into short open-

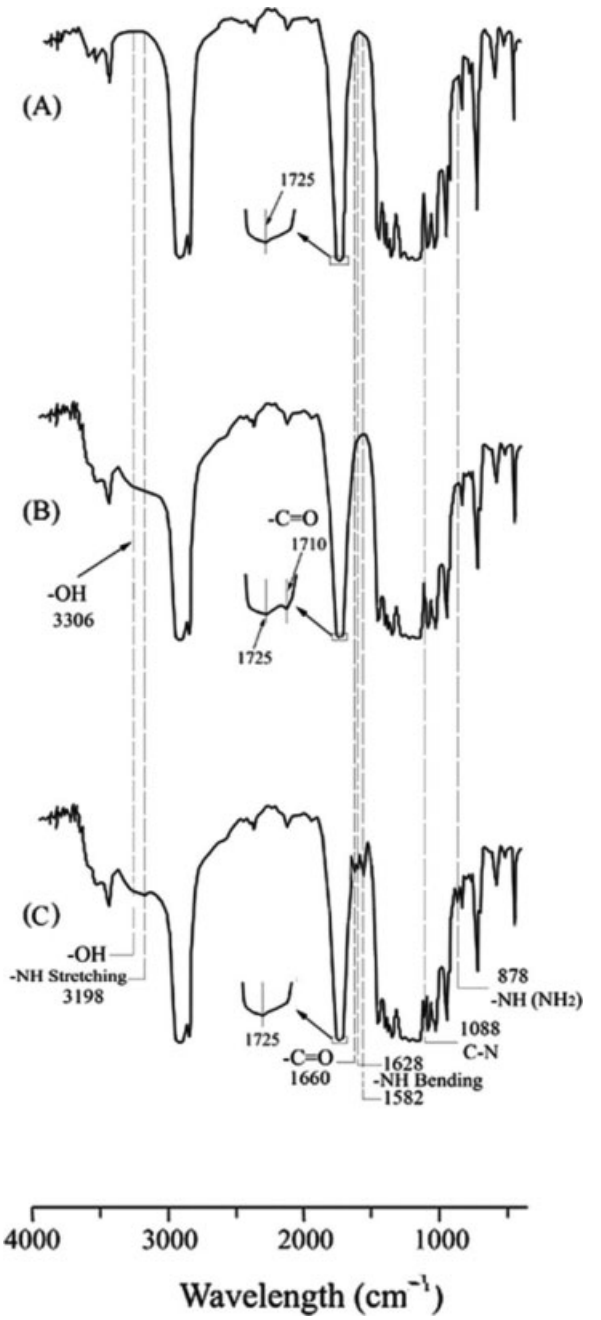

Figure 1 FTIR spectra for (A) PCL, (B) PCL-*g*-AA, and (C) PCL-*g*-NH_2.

ended pipes, producing tube ends and sidewalls covered with the oxygen-containing functional groups such as carboxyls (—COOH), carbonyls (—C=O), and hydroxyls (—OH).[27] These attached functional groups enhance the reactivity of C_{60}. Activated C_{60} was subsequently neutralized by NaOH to produce more —OH groups, and thereafter formed C_{60}—OH,[10] which was also subjected to FTIR. The spectrum [Fig. 2(C)] shows all the characteristic peaks of C_{60}—OH at 600–500 cm^{-1} (aromatic ring), 1020 cm^{-1} (C—O), 1063 cm^{-1} (C—O), 1600–1450 cm^{-1} (aromatic ring), and 3426 cm^{-1} (—OH), and is similar to that produced by Vileno et al.[10] A comparison with the FTIR spectrum of C_{60}—COOH suggests that the peaks appearing at around 1020 cm^{-1} and 1063 cm^{-1} in the spectrum of C_{60}—OH could be from the stretching vibration of —C—O in —C_{60}—OH. The results therefore confirm that —COOH group is partially converted into C_{60}—OH in the reaction involving NaOH. Further comparison of the spectra of C_{60}, C_{60}—COOH, and C_{60}—OH reveal that the hydroxyl-stretching band appeared as a strong broad band at 3296 cm^{-1} for C_{60} but shifted to 3396 and 3426 cm^{-1} for C_{60}—COOH and C_{60}—OH. The band at 3426 cm^{-1} was assigned to octahedral vacancies and designated as C_{60}—OH.

The FTIR spectra of PCL/C_{60} (5 wt %) and PCL—NH_2/C_{60}—OH (5 wt %) are shown in Figure 3(A,B), respectively. The spectrum of PCL/C_{60} (5 wt %) indicates strong absorption for aromatics in the region of 1600–1450 cm^{-1} and 600–500 cm^{-1} and this is due to the absence of a condensation reaction between PCL and C_{60}.[28,29] The spectrum of PCL—NH_2/C_{60}—OH (5 wt %), however, shows an additional unique absorption peak at 1672 cm^{-1}, similar to that seen in Figure 1(C), which is assigned to —C=O of —CONHR and is formed via the reaction between the amino of PCL—NH_2 and —OH of C_{60}—OH when the two polymers are blended. Further comparison of the spectra in Figure 3 reveals that peaks caused by —NH_2 and —OH between 3200 and 3600 cm^{-1} in PCL—NH_2/C_{60}—OH (5 wt %) are much more intense than the stretching absorbance at 3000–3600 cm^{-1} in PCL/C_{60} (5 wt %). In addition, for PCL—NH_2/C_{60}—OH (5 wt %) hybrids, the broadened peaks appearing at around 3285 and 3178 cm^{-1}

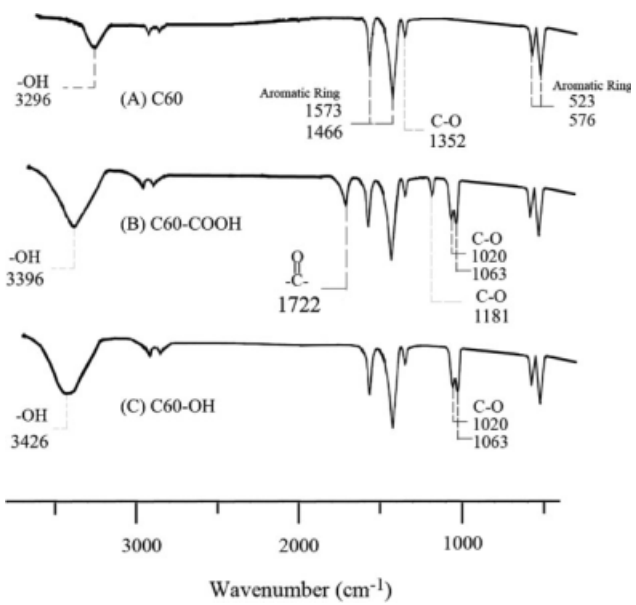

Figure 2 FTIR spectra for (A) C_{60}, (B) C_{60}—COOH, and (C) C_{60}—OH.

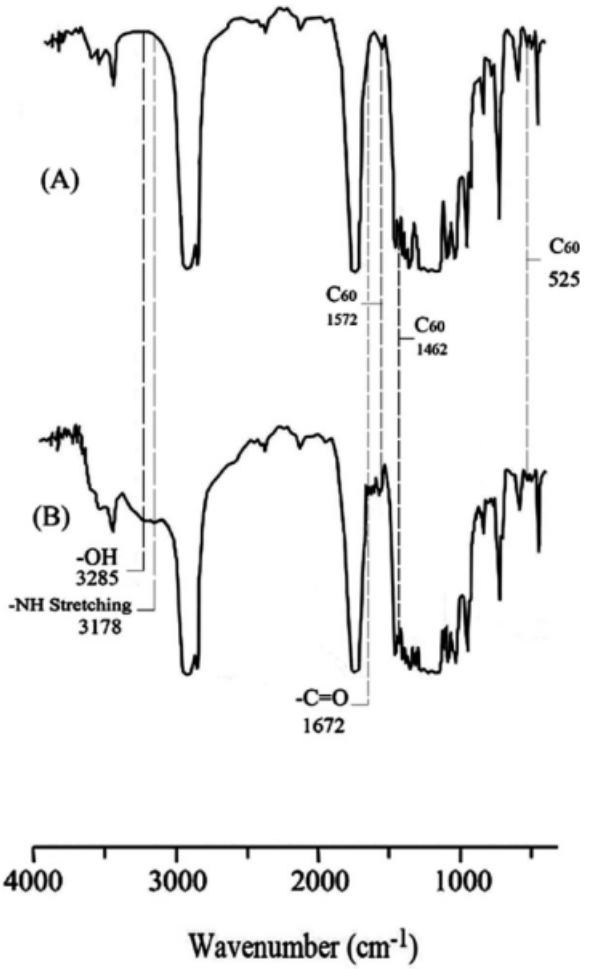

Figure 3 FTIR spectra for (A) PCL/C_{60} (5 wt %) and (B) PCL-*g*-NH_2/C_{60}—OH (5 wt %).

are attributed to the stretching vibration of —OH and —N—H groups in the C_{60}—OH and PCL—NH_2. Another contribution to the broadening in wave number is the presence of H_2O formed from the reaction between PCL—NH_2 and C_{60}—OH.

To further confirm the grafting of $-(CH_2)_2CONH(CH_2)_6NH_2$ onto PCL-*g*-AA and to investigate the compatibility between PCL—NH_2 and C_{60}—OH, ^{1}H-NMR was used to examine the structure of PCL, PCL—NH_2, and PCL—NH_2/C_{60}—OH, and the resulting spectra are shown in Figure 4. For the pure PCL [Fig. 4 (A)], ^{1}H-NMR peaks occurred in five places (1: $\Delta = 4.01$ ppm; 2: $\Delta = 1.48$ ppm; 3: $\Delta = 1.25$ ppm; 4: $\Delta = 1.59$ ppm; 5: $\Delta = 2.19$ ppm), similar to the findings of previous works.[22,30] The ^{1}H-NMR spectrum of PCL—NH_2 [Fig. 4(B)] indicated five extra peaks (6: $\Delta = 1.82$ ppm; 7: $\Delta = 2.28$ ppm; 8: $\Delta = 3.03$ ppm; 9: $\Delta = 1.41$ ppm; 10: $\Delta = 1.08$ ppm). These extra peaks confirmed that $-(CH_2)_2CONH(CH_2)_6NH_2$ had indeed been grafted onto PCL, and the corresponding structure is also presented in Figure 4(B).[31,32] Finally, the spectrum of PCL—NH_2/C_{60}—OH, shown in Figure 4(C), contains a further extra peak [11: $\Delta = 3.4$–3.5 ppm (aromatic carbon of C_{60})]. This provides evidence of the condensation between PCL—NH_2 and C_{60}—OH and suggests that the original C_{60}—OH was fully hydroxylated and that the hydroxyl groups were converted to —CONHR (also represented by FTIR peaks at 1670 cm^{-1}).

Figure 5 shows the results of ^{13}C-NMR used to examine the structure of PCL, PCL—NH_2, and PCL—NH_2/C_{60}—OH to further confirm the grafting previously proposed. For the pure PCL [Fig. 5(A)], all the characteristic carbon peaks occurred in six places (1: $\Delta = 64.21$ ppm; 2: $\Delta = 28.88$ ppm; 3: $\Delta = 25.93$ ppm; 4: $\Delta = 25.01$ ppm; 5: $\Delta = 34.26$ ppm; 6: $\Delta = 173.36$ ppm), and this was similar to the findings of Spevacek et al.[33] The ^{13}C-NMR spectrum of PCL—NH_2 [Fig. 5(B)] showed six extra peaks (7: $\Delta = 26.32$ ppm; 8: $\Delta = 36.03$ ppm; 9: —C=O $\Delta = 175.16$ ppm; 10: $\Delta = 39.48$ ppm; 11: $\Delta = 29.91$ ppm; 12: $\Delta = 27.21$ ppm). These extra peaks exactly demonstrate the grafting of $NH_2(CH_2)_6NH_2$ onto PCL—NH_2.[34–36] A comparison of the spectra of PCL—NH_2 and PCL—NH_2/C_{60}—OH [Fig. 5(C)] revealed an extra peak in the latter at $\delta = 142$–147 ppm (aromatic carbon of C_{60}) and this is due to the reaction between PCL—NH_2 and C_{60}—OH. This also verifies the full hydroxylation of C_{60}—OH and the condensation between PCL—NH_2 and C_{60}—OH.

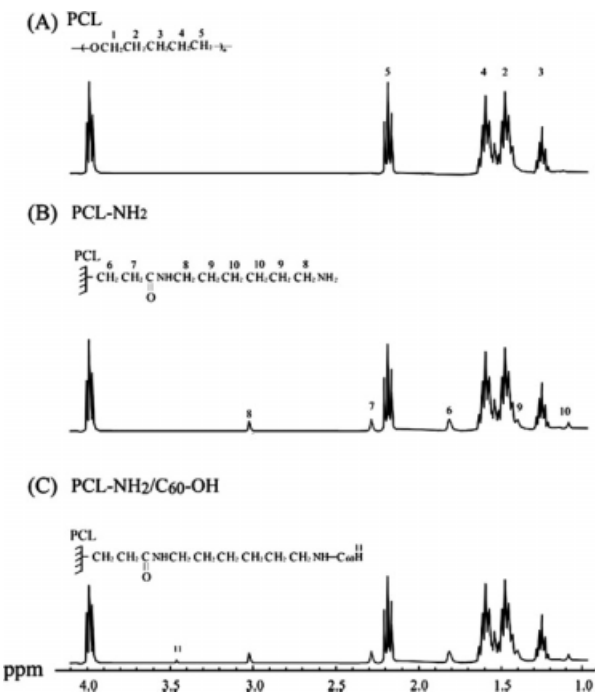

Figure 4 ^{1}H-NMR spectra for (A) PCL and (B) PCL-*g*-NH_2, and (C) PCL-*g*-NH_2/C_{60}—OH (5 wt %).

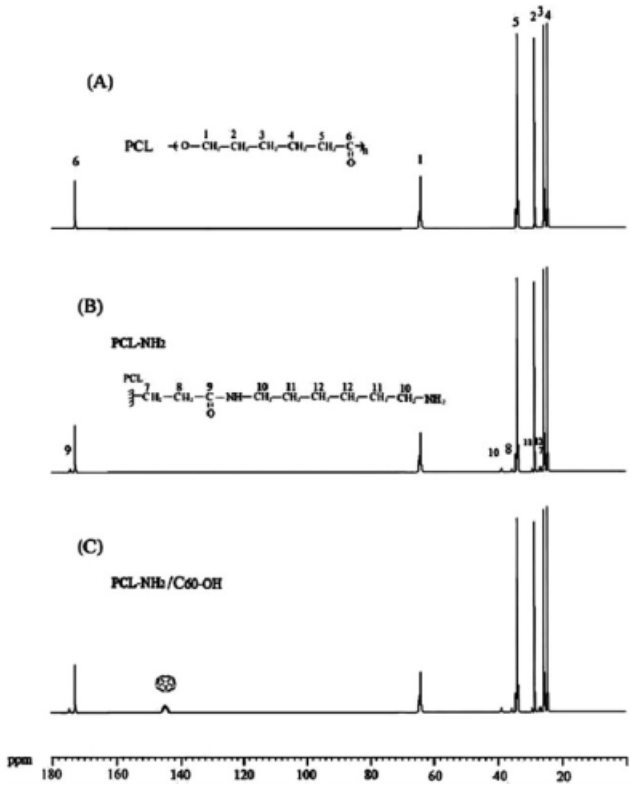

Figure 5 ^{13}C-NMR spectra for (A) PCL and (B) PCL-*g*-NH_2, and (C) PCL-*g*-NH_2/C_{60}—OH (5 wt %).

DMA analysis

The dynamic mechanical properties of PCL—NH_2 and PCL—NH_2/C_{60}—OH were measured and used to evaluate the compatibility of hybrids. Figure 6 gives the variations of the loss tangent (tan δ) with temperature for the PCL—NH_2 and PCL—NH_2/C_{60}—OH hybrids, and the results show that the tan δ increases sharply at a particular temperature when segmental motion starts. Additionally, in the case of PCL—NH_2/C_{60}—OH hybrids, the peak generally broadens and decreases in intensity with an increase of C_{60}—OH content. Moreover, because the network hinders segmental motions of the polymer chains, the damping temperature, at which a displaced maximum occurred due to the glass transition of PCL—NH_2, increased markedly from −41.8 to −31.5°C as the C_{60}—OH content was increased from 0 to 5 wt %. The shifts in tan δ to higher temperatures in the PCL—NH_2/C_{60}—OH hybrids suggested increased adhesion between the polymer and the C_{60}—OH in this system. It was also found that the damping temperature of hybrids declined with C_{60}—OH content 10 wt %, and this is because excess C_{60}—OH caused separation of the organic and inorganic phases and lowered their compatibility. It is concluded, therefore, that the most appropriate interfacial interactions occurred at approximately 5 wt % C_{60}—OH.

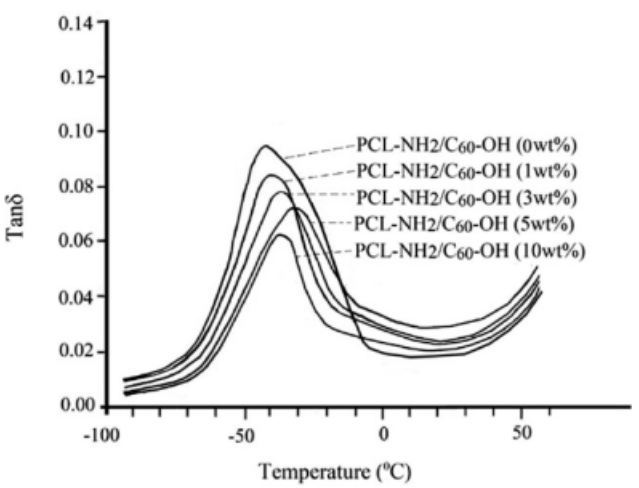

Figure 6 Variation of the tan δ with temperature for PCL-*g*-NH_2 and its blends with different contents of C_{60}—OH.

The glass transition temperatures (T_g) of PCL/C_{60} and PCL—NH_2/C_{60}—OH hybrids are summarized in Table I. As expected, both hybrids recorded a higher T_g than pure PCL or pure PCL—NH_2. It was also found that the enhancement in T_g for PCL—NH_2/C_{60}—OH hybrids was more significant than that for PCL/C_{60} hybrids. This is because the C_{60}—OH phase was able to form chemical bonds on —NH_2 sites provided by PCL—NH_2. These bonds are stronger than the hydrogen bonds in PCL/C_{60} and therefore are able to hinder the motion of the polymer chains. Furthermore, it can be seen that T_g increased with C_{60}—OH content up to 5 wt % and decreased at content above 5 wt %. The increase in T_g is due to condensation between PCL—NH_2 and C_{60}—OH, wherease the decrease is due to the separation of the organic and inorganic phases, which lowers their compatibility and T_g value.

DSC/TGA analysis

The thermal properties of hybrids with various C_{60} or C_{60}—OH contents were obtained via DSC and

TABLE I
Glass Transition Temperature of PCL/C_{60} and PCL—NH_2/C_{60}—OH Hybrids

C_{60} or C_{60}—OH (wt %)	PCL/C_{60} T_g (°C)	PCL—NH_2/C_{60}—OH T_g (°C)
0	−43.3	−41.8
1	−42.9	−39.3
3	−41.8	−36.8
5	−40.8	−31.5
7	−40.6	−33.2
10	−40.5	−36.3

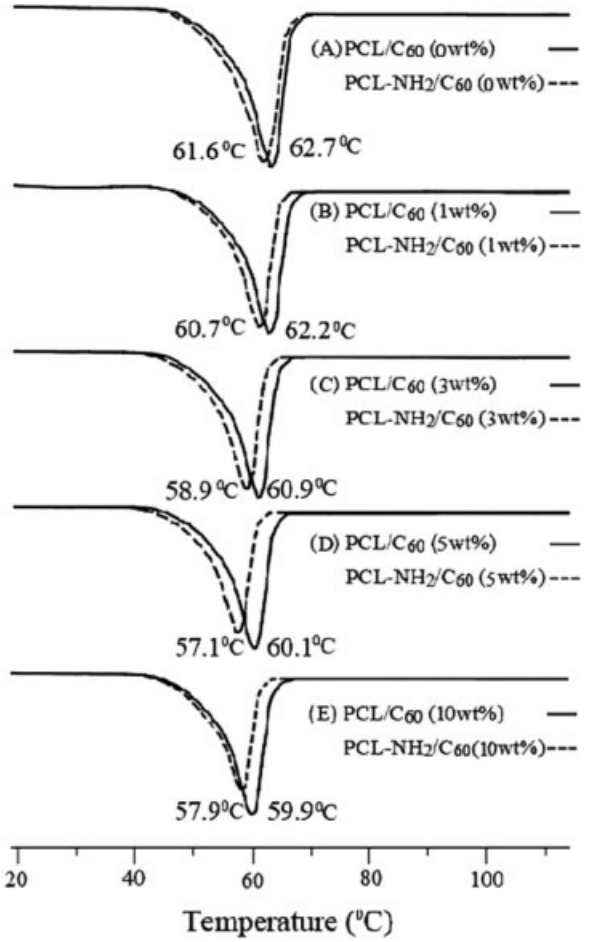

Figure 7 DSC heating thermograms for PCL/C_{60} and PCL-*g*-NH_2/C_{60}—OH and its blends with different contents of C_{60} or C_{60}—OH.

TGA tests, and the results are given in Figures 7 and 8. In addition, Tables II and III summarize the thermal and mechanical properties (T_m, ΔH_m, and IDT) of PCL/C_{60} and PCL—NH_2/C_{60}—OH hybrids. In Figure 7 and Table II, it is shown that the melting temperature (T_m) decreased with increasing C_{60} content for PCL/C_{60}, whereas for PCL—NH_2/C_{60}—OH, the lowest T_m occurred at 5 wt % of C_{60}—OH. Moreover, T_m values for all PCL—NH_2/C_{60}—OH hybrids were lower than their PCL/C_{60} equivalents. This lower melting temperature of PCL—NH_2/C_{60}—OH makes it a more easily processed blend.

Table II shows that the values of melting heat (ΔH_m) of pure PCL and PCL-*g*-AA are 72.5 ± 1.1 J/g and 69.5 ± 1.1 J/g, respectively. The lower melting heat for PCL-*g*-AA, when compared with pure PCL, increased the spacing between the chains probably due to the grafted branches that disrupted the regularity of the chain structures in PCL. It can be seen from Table II that the corresponding ΔH_m values of PCL/C_{60} hybrids having C_{60} contents of 1, 3, 5, 7, and 10 wt % are 64.8 ± 1.0 J/g, 55.2 ± 0.9 J/g, 44.6 ± 0.9 J/g, 41.6 ± 0.7 J/g, and 38.3 ± 0.6 J/g. For the PCL-*g*-AA/C_{60}—OH hybrids with 1, 3, 5, 7, and 10 wt % C_{60}—OH, the corresponding values of ΔH_m are 67.6 ± 1.0 J/g, 62.8 ± 1.0 J/g, 57.8 ± 0.9J/g, 53.6 ± 0.8 J/g, and 49.3 ± 0.7 J/g. It is clear that the ΔH_m values of PCL/C_{60} and PCL-*g*-AA/C_{60}—OH, which suggest the melting heat (ΔH_m) decreased as the C_{60} or C_{60}—OH content increased. These carbons inhibit the movement of the polymer segments, and therefore increased levels probably acted to prevent crystal formation, which in turn lowered the ΔH_m. Another potential cause of changes in ΔH_m is the condensation reaction character of C_{60} and C_{60}—OH, increased levels of which lead to poor adhesion with the polymer. Additionally, ΔH_m was about 3–13 J/g higher with PCL—NH_2 in the composite in place of PCL. This higher ΔH_m was caused by the formation of the amide functional group from the reaction between the —OH group of C_{60}—OH and the —NH_2 group of PCL—NH_2.

It is known that the defunctionalization of C_{60}—OH can be realized by thermal decomposition. In this study, thermal gravimetry analysis (TGA) was used to determine the effect of C_{60}—OH content on the weight loss of hybrids, and the results are presented in Figure 8 and Table II. Both PCL/C_{60} and PCL—NH_2/C_{60}—OH hybrids were seen to have higher IDT values than pure PCL and pure PCL—NH_2 (Table II). This raised IDT was probably caused by increased difficulty in arranging the polymer chain due to the already noted prohibition of movement of polymer segments by C_{60} or C_{60}—OH. Similarly, another potential cause is the condensation reaction, which leads to increased adhesion of C_{60}—OH with PCL—NH_2. Xiao et al.[37] studied the properties of poly(phenylenevinylene)/C_{60} composites and reported similar phenomena. Noticeably, despite PCL—NH_2 having a lower IDT value than

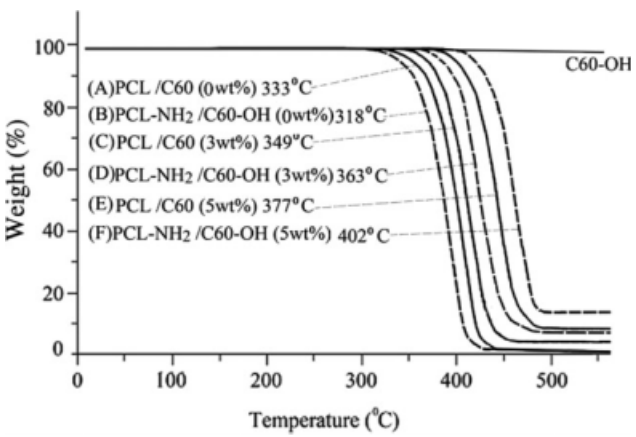

Figure 8 TGA curves for PCL/C_{60} and PCL-*g*-NH_2/C_{60}—OH and its blends with different contents of C_{60} or C_{60}—OH.

TABLE II
Thermal Properties of PCL/C_{60} and PCL—NH_2/C_{60}—OH Hybrids

C_{60} or C_{60}—OH (wt %)	PCL/C_{60}			PCL—NH_2/C_{60}—OH		
	IDT (°C)	ΔH_m (J/g)	T_m (°C)	IDT (°C)	ΔH_m (J/g)	T_m (°C)
0	333	72.5 ± 1.1	62.7	318	69.5 ± 1.1	61.6
1	340	64.8 ± 1.0	62.2	351	67.6 ± 1.0	60.7
3	349	55.2 ± 0.9	60.9	363	62.8 ± 1.0	58.9
5	377	44.6 ± 0.9	60.1	402	57.8 ± 0.9	57.1
7	381	41.6 ± 0.7	60.0	412	53.6 ± 0.8	57.5
10	385	38.3 ± 0.6	59.9	420	49.3 ± 0.7	57.9

PCL, the PCL—NH_2/C_{60}—OH hybrids produced IDT values higher than those of the equivalent PCL/C_{60}. This outcome is a result of the difference in interfacial forces in the two hybrids: the weaker hydrogen bonds of PCL/C_{60} compared with the stronger coordination sites associated with the amide groups of PCL—NH_2/C_{60}—OH. Table II also shows that the increment of IDT for both hybrids was insignificant with C_{60} or C_{60}—OH content above 5 wt %. For example, the increment of IDT is about 84°C for 5 wt % C_{60}—OH but it is only 26°C as the C_{60}—OH content is increased from 5 to 10 wt %. This was because of the formation of agglomerates at higher filler content and is a result that further confirmed the optimal loading of C_{60}—OH as 5 wt %.

Residual yields of PCL—NH_2/C_{60}—OH composites were seen to increase with increasing C_{60}—OH content (Fig. 8). This result may be attributed to a physical barrier effect, resulting from the fact that C_{60}—OH prevents the transport of decomposition products in the polymer composites. This effect, produced by ablative reassembling of a C_{60} layer, was reported as improving the thermal stability of polypropylene/MWNTs nanocomposites.[38] Furthermore, residual yields were about 3–8% higher with PCL—NH_2/C_{60}—OH in the composite in place of PCL/C_{60}. Higher residual yields are caused by the formation of an amide functional group. Hence, the TGA results demonstrate that the incorporation of a small quantity of C_{60}—OH can significantly improve the thermal stability of the PCL—NH_2/C_{60}—OH composites.

TABLE III
Mechanical Properties of PCL/C_{60} and PCL—NH_2/C_{60}—OH Hybrids

C_{60} or C_{60}—OH (wt %)	PCL/C_{60}	PCL—NH_2/C_{60}—OH
	TS (MPa)	TS (MPa)
0	37.6 ± 0.7	35.8 ± 0.8
1	38.1 ± 0.9	41.5 ± 1.0
3	39.3 ± 1.1	46.2 ± 1.2
5	40.5 ± 1.2	53.6 ± 1.3
7	39.9 ± 1.1	50.5 ± 1.2
10	38.6 ± 1.0	43.5 ± 1.0

Figure 8 also shows that neat C_{60}—OH did not degrade even at temperatures above 500°C. This observation supports the conclusion that weight loss of the composites is due to the decomposition of PCL—NH_2 and confirms that weight loss percent of PCL—NH_2/C_{60}—OH decreases with increasing C_{60}—OH content.

Figure 9(A) shows an SEM image of PCL/C_{60} after it was subjected to TGA up to 450°C. The amorphous PCL covering the C_{60} (5 wt %) faded after

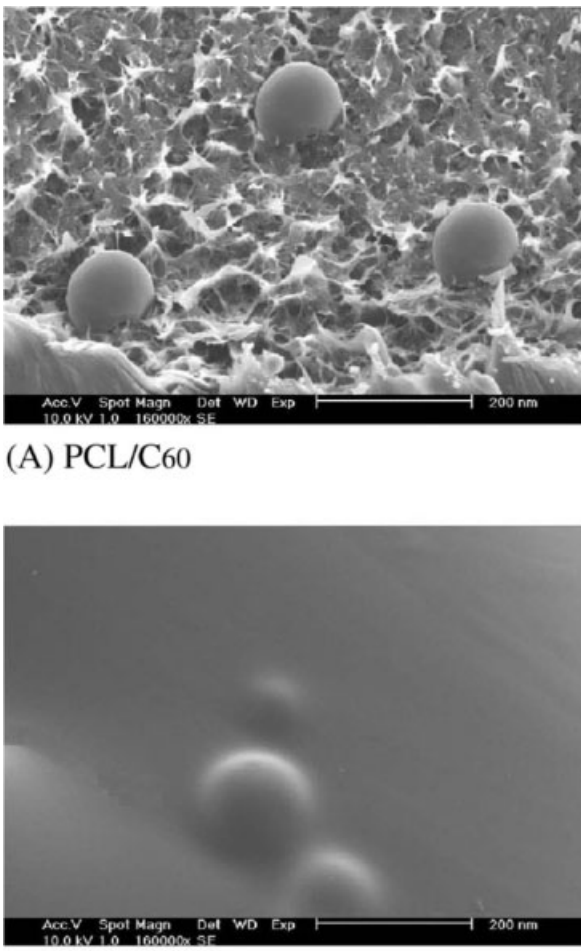

Figure 9 SEM micrographs of PCL/C_{60} (5 wt %) and PCL-*g*-NH_2/C_{60}—OH (5 wt %) subjected to TGA at 450°C.

being heated to 450°C, although some residual was observed, suggesting that the PCL was not covalently bonded to the walls of C_{60}. Conversely, there was no degradation observed for PCL—NH_2 and C_{60}—OH [Fig. 9(B)], demonstrating that these molecules were covalently bonded during the blending process.

Hybrid morphology

It is necessary to study the morphology of PCL/C_{60} and PCL—NH_2/C_{60}—OH blends since the mechanical properties depend on it. For the blends in this study, the major component (PCL or PCL—NH_2) forms the matrix, whereas the minor component (C_{60} or C_{60}—OH) is the dispersed phase. In general, a good dispersion of filler (C_{60} or C_{60}—OH) in the polymer matrix, effective functional groups of filler (e.g. —OH of C_{60}—OH), and strong interfacial adhesion between the two phases are required to obtain a composite material with satisfactory mechanical properties. SEM was used to study the tensile fractured surfaces of PCL/C_{60} (5 wt %) and PCL—NH_2/C_{60}—OH (5 and 10 wt %) blends, and the SEM microphotographs are shown in Figure 10. It may be supposed that a lack of wettability may lead to some agglomerated C_{60} clusters. Figure 10(A) shows poor wetting of C_{60} for the PCL/C_{60} hybrid, and the reason for this is the large difference in the surface energy between C_{60} and the PCL matrix. Conversely, entangled clusters were not seen on the fractured surface of the PCL—NH_2/C_{60}—OH hybrid [Fig. 10(B)]. Also, smooth interfaces were observed between the PCL—NH_2-embedded C_{60}—OH, hence C_{60}—OH is considered to have good wettability with PCL—NH_2. All these findings illustrate the wettability of C_{60}—OH in PCL—NH_2. In terms of wt %, C_{60}—OH was easily dispersed well in the polymer matrix for 5 wt % of C_{60}—OH, whereas the formation of agglomerates was observed at 10 wt % [Fig. 10(C)]. Likewise, good dispersion of PCL—NH_2/C_{60}—OH (5 wt %) and the formation of agglomerates for PCL—NH_2/C_{60}—OH (10 wt %) is observable in the TEM micrographics in Figure 11(A,B). The phenomenon of agglomeration may be due to condensation of C_{60}—OH at higher contents.

Mechanical properties of hybrids

The stress–strain curves of the PCL/C_{60} and PCL—NH_2/C_{60}—OH composites with different C_{60} or C_{60}—OH content are shown in Figure 12 and Table III. In all cases the curves are linear at low strain followed by plastic deformation in the region of 380% strain. At higher strains, up to 630% for the PCL—NH_2, the films yielded a breaking strain. This breaking strain tended to decrease with increasing

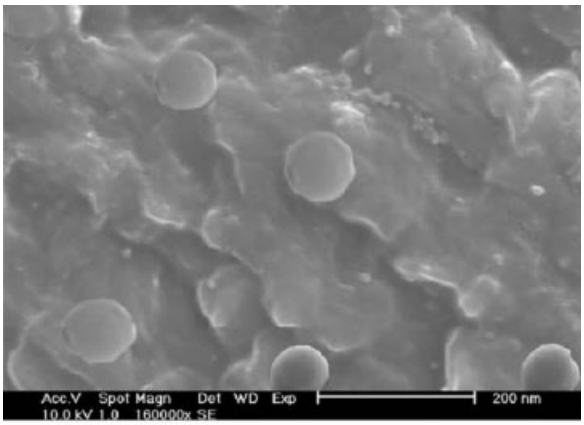

(A) PCL/C_{60} (5 wt%)

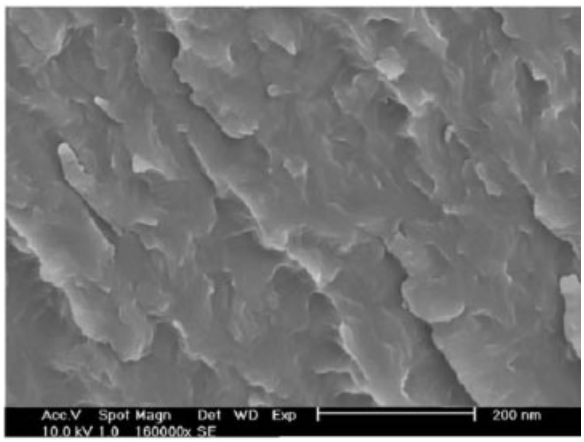

(B) PCL-NH_2/C_{60}-OH (5 wt%)

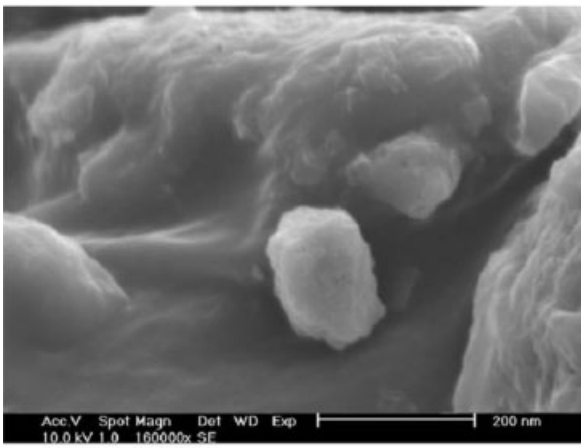

(C) PCL-NH_2/C_{60}-OH (10 wt%)

Figure 10 SEM micrographs of tensile fracture surfaces of (A) PCL/C_{60} (5 wt %), (B) PCL-*g*-NH_2/C_{60}—OH (5 wt %), and (C) PCL-*g*-NH_2/C_{60}—OH (10 wt %).

C_{60}—OH content and occurred at approximately 400% for the 5 wt % composite followed by a stiffening of the material.[38,39] Tensile strength of the composites is shown in Table III and Figure 12. For PCL/C_{60} hybrids, it is clear that the effect of C_{60} content on the tensile strength is somewhat insignificant because of the relatively weak hydrogen bond-mediated interfacial force between the PCL matrix and the C_{60}. PCL—NH_2/C_{60}—OH hybrids exhibited much better tensile strength than the equivalent PCL/C_{60}, despite PCL—NH_2 having a lower tensile strength than pure PCL. The enhancement in tensile strength was attributed to the presence of the C_{60}—OH and the consequent formation of chemical bonds, through the condensation reaction with amino groups in PCL—NH_2. However, after increasing rapidly with the increase of C_{60}—OH from 0 to 5 wt %, the tensile strength of PCL—NH_2/C_{60}—OH hybrids declined with further increases in wt % (Table III). In addition to chemical bonds formed in the hybrids, the positive effect on tensile strength may be due to the stiffness of the C_{60}—OH layers, which contributes to the presence of immobilized or partially immobilized polymer phases[40] and to high aspect ratio and surface area of the C_{60}—OH layers dispersed in the polymer matrix. It is also possible that C_{60}—OH layer orientation as well as molecular orientation contribute to the observed reinforcement effect. The slight decline in tensile strength for the C_{60}—OH content above 5 wt % could be attributed to the inevitable aggregation of C_{60}—OH in high C_{60}—OH content blends. These results support the theoretical and molecular simulation predictions that stress transfer, and hence strength, of C_{60}–polymer composites can be effectively increased by the formation of chemical bonding between them.[19,41,42]

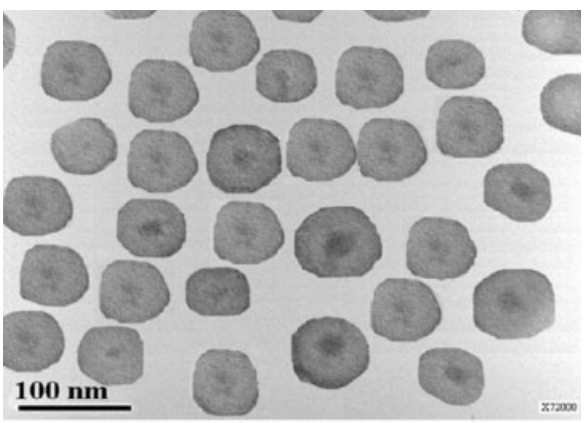

Figure 11 TEM micrographs of (A) PCL-*g*-NH_2/C_{60}—OH (5 wt %) and (B) PCL-*g*-NH_2/C_{60}—OH (10 wt %).

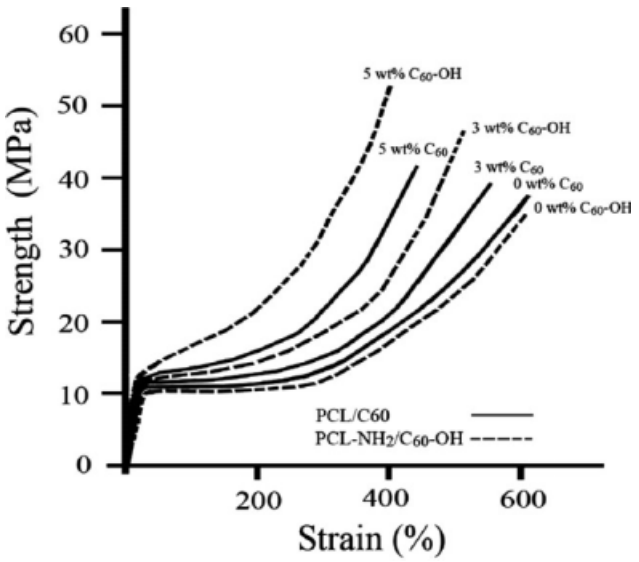

Figure 12 Representative stress–strain curves for PCL/C_{60} and PCL-*g*-NH_2/C_{60}—OH-based composites for a range of C_{60} or C_{60}—OH content.

CONCLUSIONS

In this study, we synthesized and characterized a PCL/C_{60} and PCL—NH_2/C_{60}—OH composite. The modification of C_{60} involved a chemical oxidation to cleave C_{60} and to open the C_{60} ends, creating hydroxyl functionalities on the C_{60}. This provided the C_{60} with a very effective side chain, enabling the C_{60}—OH to play a reinforcement role in the PCL—NH_2 polymer matrix. FTIR and solid-state ^{1}H- and ^{13}C-NMR spectra showed that the amino groups had been grafted onto the PCL copolymer and that amide bonds had formed in the PCL—NH_2/C_{60}—OH hybrid. The newly formed amide bonds may be produced through dehydration of amino groups in the PCL—NH_2 matrix with hydroxyl groups in the C_{60}—OH. SEM microphotographs showed that the wettability of C_{60}—OH in PCL—NH_2 was much better than the wettability of C_{60} in PCL, implying that the compatibility between PCL and C_{60} had been enhanced in the former. Moreover, the formation of

agglomerates of C_{60}—OH was observed for hybrids with higher C_{60}—OH content using TEM examination. TGA tests showed that the PCL—NH_2/C_{60}—OH hybrid with 5 wt % C_{60}—OH gave an increment of 84°C for the IDT. Maximum values of tensile strength of hybrid occurred at about 5 wt % of C_{60}—OH. The compatibility of hybrid was reduced above this wt % due to the inevitable aggregation of C_{60}.

References

1. Arias-Marin, E.; Moigne, J. L.; Maillou, T.; Guillon, D.; Moggio, I.; Geffroy, B. Macromolecules 2003, 36, 3570.
2. Wang, M.; Pramoda, K. P.; Goh, S. H. Chem Mater 2004, 16, 3452.
3. Mwaura, J. K.; Pinto, M. R.; Witker, D.; Ananthakrishnan, N.; Schanze, K. S.; Reynolds, J. R. Langmuir 2005, 21, 10119.
4. Kawauchi, T.; Kumaki, J.; Yashima, E. J Am Chem Soc 2005, 127, 9950.
5. Tang, Z.; Padmawar, P. A.; Canteenwala, T.; Gao, Y.; Watkins, E.; Majewski, J.; Chiang, L. Y.; Wang, H. L. Langmuir 2006, 22, 5366.
6. Gayathri, S. S.; Agarwal, A. K.; Suresh, K. A. Langmuir 2005, 21, 12139.
7. Ren, S.; Yang, S.; Zhao, Y. Langmuir 2004, 20, 3601.
8. Sun, Y. P.; Lawson, G. E.; Bunker, C. E.; Johnson, R. A.; Ma, B.; Farmer, C.; Riggs, J. E.; Kitaygorodskiy, A. Macromolecules 1996, 29, 8441.
9. Song, T.; Goh, S. H.; Lee, S. Y. Macromolecules 2002, 35, 4133.
10. Vileno, B.; Marcoux, P. R.; Lekka, M.; Sienkiewicz, A.; Feher, T.; Forro, L. Adv Funct Mater 2006, 16, 120.
11. Huang, X. D.; Goh, S. H.; Lee, S. Y. Macromol Chem Phys 2000, 201, 2660.
12. Chen, Y.; Zhao, Y.; Cai, R.; Huang, Z. E.; Xiao, L. J Polym Sci Part B: Polym Phys 1998, 36, 2653.
13. Wu, H.; Li, F.; Lin, Y.; Yang, M.; Chen, W.; Cai, R. J Appl Polym Sci 2006, 99, 828.
14. Komatsu, K.; Murata, Y.; Takimoto, N.; Mori, S.; Sugita, N.; Wan, T. S. M. J Org Chem 1994, 59, 6101.
15. Berrada, M.; Hashimoto, Y.; Miyata, S. Chem Mater 1994, 6, 2023.
16. Huang, X. D.; Goh, S. H.; Lee, S. Y.; Huan, C. H. A. Macromol Chem Phys 2000, 201, 281.
17. Yoon, K. R.; Kim, W. J.; Choi, I. S. Macromol Rapid Commun 2004, 205, 1218.
18. Thess, A.; Lee, R.; Nikoaev, P.; Dai, H.; Robert, J.; Xu, C.; Lee, Y. H.; Kim, S. G.; Rinzler, A. G.; Colbert, D. T.; Scuseria, G. E.; Tomanek, D.; Fisher, J. E.; Smalley, R. E. Science 1996, 273, 483.
19. Ma, C. C. M.; Sung, S. C.; Wang, F. Y.; Chiang, L. Y.; Wang, L. Y.; Chiang, C. L. J Polym Sci Part B: Polym Phys 2001, 39, 2436.
20. Ishida, H.; Lee, Y. H. Polymer 2001, 42, 6971.
21. Chen, B.; Sun, K. Polym Test 2005, 24, 978.
22. Wu, C. S. Polym Degrad Stab 2003, 80, 127.
23. Laurienzo, P.; Martuscelli, E.; Raimo, M.; Rimedio, R. Polymer 2000, 16, 3875.
24. Wu, C. S. Polymer 2005, 46, 147.
25. Zong, Z.; Kimura, Y.; Takahashi, M.; Yamane, H. Polymer 2000, 41, 899.
26. Huang, H. M.; Lin, I. C.; Chang, C. Y.; Tsai, H. C.; Hsu, C. H.; Tsiang, R. C. J Polym Sci Part A: Polym Chem 2004, 42, 5802.
27. Kuznetsova, A.; Mawhinney, D. B.; Naumenko, V.; Yates, J. T., Jr.; Li, Q.; Smalley, R. E. J Phys Chem B 2000, 321, 292.
28. Yu, J.; Zhang, Z.; Ni, Y.; Lu, Y.; Xiong, Y.; Xu, W. J Appl Polym Sci 2007, 105, 821.
29. Cataldo, F. H. Polym Int 1999, 48, 143.
30. He, A.; Han, C. C.; Yang, G. Polymer 2004, 45, 8231.
31. Pham, O. T.; Petiaud, R.; Waton, H.; Liauro-Darricades, M.-F. Proton and Carbon NMR Spectra of Polymers; Penton Press: London, 1991; p 89.
32. Li, Z.; Shao, P.; Qin, J. J Appl Polym Sci 2004, 92, 867.
33. Spevacek, J.; Brus, J.; Divers, T.; Grohens, Y. Eur Polym J 2007, 43, 1866.
34. Jeong, J. H.; Kang, H. S.; Yang, S. R.; Kim, J. D. Polymer 2003, 44, 583.
35. Wu, Q.; Yoshino, T.; Sakabe, H.; Zhang, H.; Isobe, S. Polymer 2003, 44, 3909.
36. Li, Z.; Qin, J.; Xu, X. J Polym Sci Part A: Polym Chem 2004, 42, 2877.
37. Xiao, S.; Wang, S.; Fang, H.; Li, Y.; Shi, Z.; Du, C.; Zhu, D. Macromol Rapid Commun 2001, 22, 1313.
38. Jin, W.; Kader, M. A.; Ko, W.-B.; Nah, C. Polym Adv Technol 2004, 15, 662.
39. Zhang, X.; Liu, T.; Sreekumar, T. V.; Kumar, S.; Moore, V. C.; Hauge, R. H.; Smalley, R. E. Nano Lett 2003, 3, 1285.
40. Coleman, J. N.; Cadek, M.; Blake, R.; Nicolosi, V.; Ryan, K. P.; Belton, C.; Fonseca, A.; Nagy, J. B.; Cun'ko, Y. K.; Blau, W. J. Adv Funct Mater 2004, 14, 791.
41. Liu, L.; Barber, A. H.; Nuriel, S.; Wagner, H. D. Adv Funct Mater 2005, 15, 975.
42. Gunji, T.; Sakai, Y.; Arimitsu, K.; Abe, Y. J Polym Sci Part A: Polym Chem 2007, 45, 3273.